JMEPEG (2012) 21:1374–1379
DOI: 10.1007/s11665-011-0010-5

1059-9495/$19.00

A Nanocrystalline $Ni_2(Cr,Mo)$ Intermetallic with Potentially Useful Combination of Properties for Gas Turbine Seal Ring Applications

H.M. Tawancy and Luai M. Al-Hadhrami

(Submitted January 10, 2011; in revised form June 17, 2011)

Seal rings are installed for each turbine stage in gas turbine engines to minimize the loss in gas pressure and maintain engine efficiency. During service, seal rings become susceptible to failure by thermal fatigue as demonstrated by a case study. Therefore, a lower coefficient of thermal expansion is among the most important requirements for these applications. We show that long-range ordering in a Ni-Cr-Mo alloy can be used to synthesize a nanocrystalline intermetallic compound combining high strength, high ductility, low coefficient of thermal expansion, and an adequate oxidation resistance up to at least 700 °C. Twinning rather than slip is found to be the predominant deformation mechanism of the intermetallic compound, which is correlated with the crystallography of the disorder-to-order transformation and microstructure evolution. This could explain the enhanced plasticity of the intermetallic compound. The combination of enhanced plasticity, low-thermal expansion, and nano-sized crystals is expected to improve the resistance to thermal fatigue failure.

Keywords electron microscopy, heat resistant metals, intermetallics

1. Introduction

To minimize the loss in gas pressure between the blades and casing of a gas turbine engine maintaining engine efficiency, a seal ring is installed for each turbine stage. During engine operation, the tips of the blades rotate in close proximity with the seal rings. Most of these seals are designed as part of a brazed honeycomb assembly where abradable materials are brazed to the seal rings (Ref 1-3). Usually, during service, seal materials are exposed to temperatures below 800 °C.

A low coefficient of thermal expansion is a primary material requirement for gas turbine seal ring applications because it serves two important functions. First, it allows for a reduced clearance between the blades and the ring; therefore, less gas can bypass the blades, which improves engine efficiency. Second, it reduces the susceptibility to thermal fatigue failure, which arises from the rapid thermal cycling encountered during engine operation. Other important properties include high-temperature strength, environmental resistance, and microstructural stability. Although intermetallic compounds possess a potentially useful combination of properties for these applications, their usefulness as structural materials is rather limited by poor ductility, e.g., (Ref 4). In recent years, however, the number of intermetallic compounds discovered to have relatively high ductility continues to increase (Ref 5, 6).

It is the objective of this article to demonstrate that long-range ordering can be used to synthesize a nanostructured $Ni_2(Cr,Mo)$ intermetallic with potentially useful combination of properties for gas turbine seal ring applications. A case study is used to illustrate the susceptibility of seal ring materials to failure by thermal fatigue.

2. Experimental Procedure

On an atomic concentration basis, the alloy included in the study had a composition of Ni-18.5% Mo-15.1% Cr approaching the $Ni_2(Cr,Mo)$ composition (Ni-26.97% Mo-11.95% Cr in wt.%). The alloy was prepared by vacuum induction melting and electro slag re-melting followed by forging, hot rolling, and then cold rolling to sheets about 1.5 mm in thickness. Specimens were solution annealed at 1065 °C for 15 min and then water quenched. Henceforth, this will be referred to as the annealed condition. Long-range ordering was induced by thermal aging at 700 °C for up to 100 h. Tensile tests were carried out at room temperature on standard samples with a gage length of 50.8 mm. Standard tests were used to measure the linear coefficient of thermal expansion at temperatures in the range of room temperature to 700 °C. Also, oxidation tests were carried out at 700 °C for up to 100 h of exposure in air with an 8 h cycling period to room temperature. Light optical metallography and electron-optical techniques including scanning electron microscopy (SEM: JEOL 5800LV) and transmission electron microscopy (TEM: JEOL 2000EX) combined with micro-

H.M. Tawancy and **Luai M. Al-Hadhrami**, Center for Engineering Research and Center of Research Excellence in Corrosion, Research Institute, King Fahd University of Petroleum & Minerals, P. O. Box 1639, Dhahran 31261, Saudi Arabia. Contact e-mail: tawancy@kfupm.edu.sa.

chemical analysis by energy dispersive x-ray spectroscopy were used to characterize the microstructure.

3. Experimental Results and Discussion

3.1 Case Study: Failure of a Gas Turbine Seal Ring by Thermal Fatigue

Figure 1 summarizes the results of a case study involving a seal ring material made of a Ni-16Cr-15Mo alloy brazed to a honeycomb made of a Ni-22Cr-18.5Fe-9 Mo alloy all in wt.%. During regular maintenance, cracks were detected in the seal ring.

A section of the seal ring assembly is shown in the photograph of Fig. 1(a). After removal of the honeycomb, cracks were detected in the seal ring as shown in the macrograph of Fig. 1(b). Light optical metallography revealed that the cracks were of the transgranular type as shown in the example of Fig. 1(c). As can be seen, the crack extends from the surface inward. A secondary electron SEM image illustrating the morphology of exposed surface of the crack is shown in Fig. 1(d). Although, details of the surface morphology were masked by oxide scale, fatigue striations could be distinguished after descaling as indicated in the marked areas of Fig. 1(d).

It could be concluded from the above observations that thermal fatigue was the most probable mode of failure. As shown below, the nanostructured $Ni_2(Cr,Mo)$ intermetallic could have improved resistance to fatigue in addition to other useful properties for seal ring applications.

3.2 Microstructure of $Ni_2(Cr,Mo)$ Alloy in the Annealed Condition (Short-Range Ordered)

Figure 2 illustrates characteristic microstructural features of the $Ni_2(Cr,Mo)$ alloy in the annealed condition with face-centered cubic (fcc) structure. A typical grain structure is shown in the light optical micrograph of Fig. 2(a). As can be seen, the material consisted of equi-axed grains with a high density of annealing twins indicating full recrystallization. It is known that a high density of annealing twins in a fcc material as shown in Fig. 2(a) reflects a relatively low stacking fault energy (Ref 7), which could have an important effect on the deformation mechanism as shown later.

Although no specific microstructural features could be distinguished on the scale of TEM, weak intensity maxima were observed at {1 1/2 0} and all equivalent positions in electron diffraction patterns as shown in the ⟨001⟩ pattern of the fcc structure (Fig. 2b). This is typical of short-range ordering in Ni-Mo-based alloys (Ref 8, 9). On thermal aging at 700 °C, the individual grains observed in Fig. 2(a) were found to be subdivided into nanoscale-ordered crystals of a Pt_2Mo-type superlattice with potentially useful combination of properties as demonstrated below.

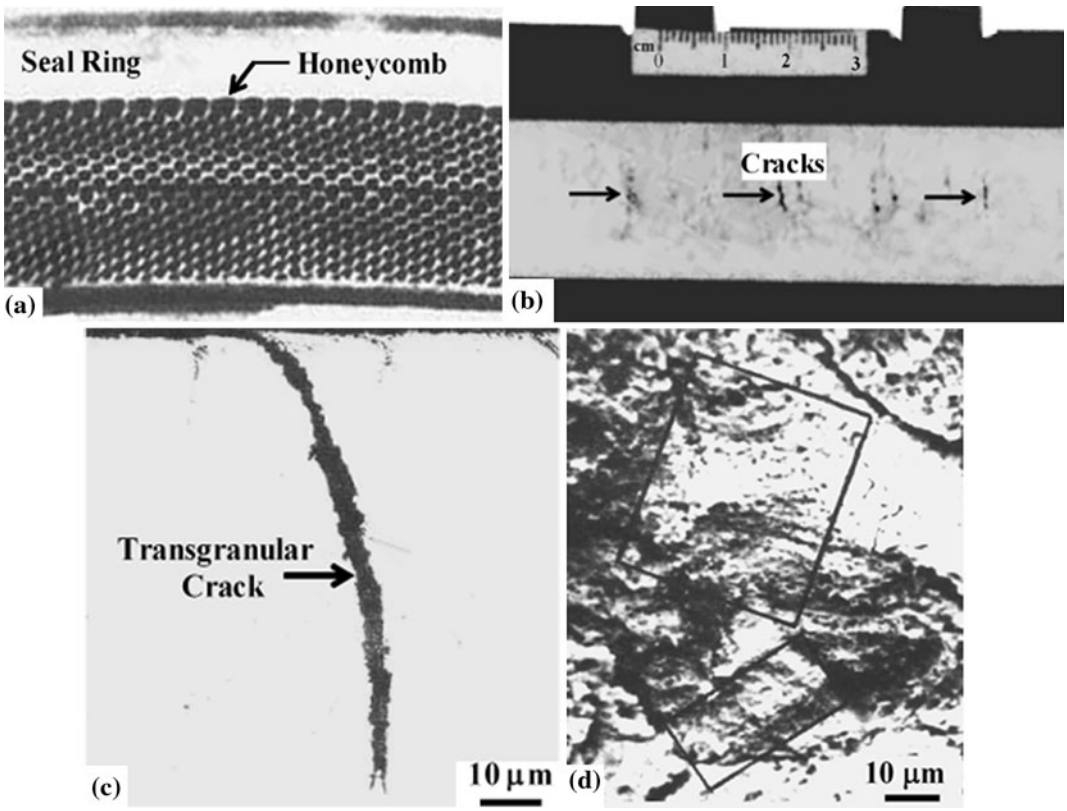

Fig. 1 A summary of a case study showing thermal fatigue as a mode of failure of a gas turbine seal ring. (a) A photograph of the brazed honeycomb assembly of the seal ring. (b) A macrograph of the seal ring after removal of the honeycomb showing cracks as indicated by the arrows. (c) A light optical micrograph along a cross section of the seal ring (as-polished) showing a transgranular crack extending from the surface inward. (d) A secondary electron SEM image illustrating the morphology of exposed surface of the crack after descaling; fatigue striation can be distinguished within the marked areas

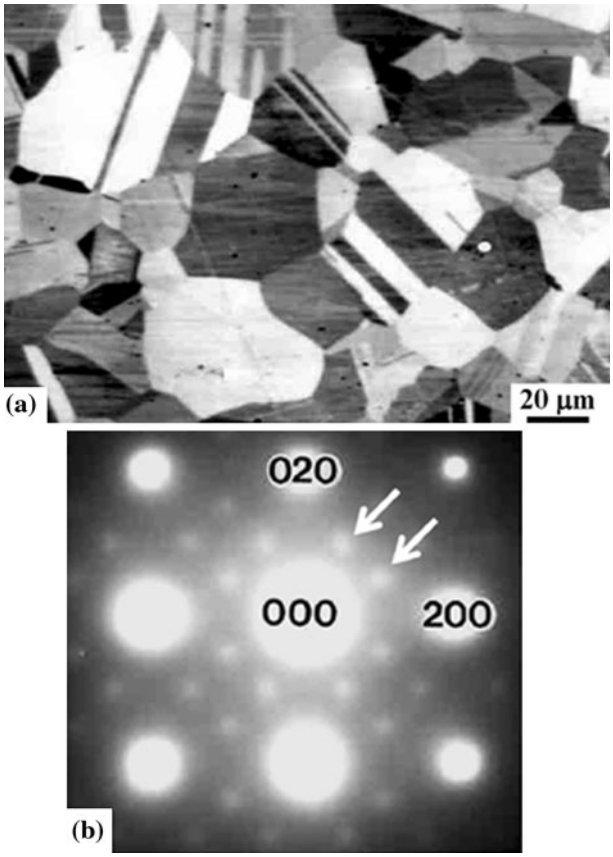

Fig. 2 Characteristic microstructural features of the $Ni_2(Cr,Mo)$ alloy in the annealed condition. (a) Light optical micrograph illustrating the grain structure with high density of annealing twins. (b) ⟨001⟩ selected area electron diffraction pattern showing short-range order reflections at {1 1/2 0} and all equivalent positions as indicated by the arrows

3.3 Microstructure of $Ni_2(Cr,Mo)$ Alloy in the Long-Range Ordered State

A bright-field TEM image across a grain boundary of the parent fcc structure after 24 h of aging at 700 °C is shown in Fig. 3(a). It is observed that both grains exhibit a "mottled" contrast characteristic of high volume fraction of ultrafine particles.

Corresponding electron diffraction patterns derived from a single grain in different orientations are shown in Fig. 3(b)-3(e). In comparison with the annealed condition (Fig. 2b), the short-range reflections were replaced by superlattice reflections at 1/3{420} positions or equivalently at 1/3{220} positions characterizing a Pt_2Mo-type superlattice. As shown in the schematic of Fig. 3(f), the Pt_2Mo-type superlattice with body-centered orthorhombic structure can directly be derived from the parent fcc structure by minor atoms rearrangement on {420} planes such that every third plane becomes occupied with Mo/Cr atoms and planes in-between contain only Ni atoms giving rise to the observed superlattice reflections at 1/3{420} positions.

Although Ni_2Mo is thermodynamically metastable in the binary Ni-Mo system (Ref 8, 9), it can be stabilized by the additions of Cr and is stable in the Ni-Mo-Cr system. Crystallographically, there are six equivalent variants of the Pt_2Mo-type superlattice, i.e., during the transition from short-range to long-range ordering, each grain of the parent fcc

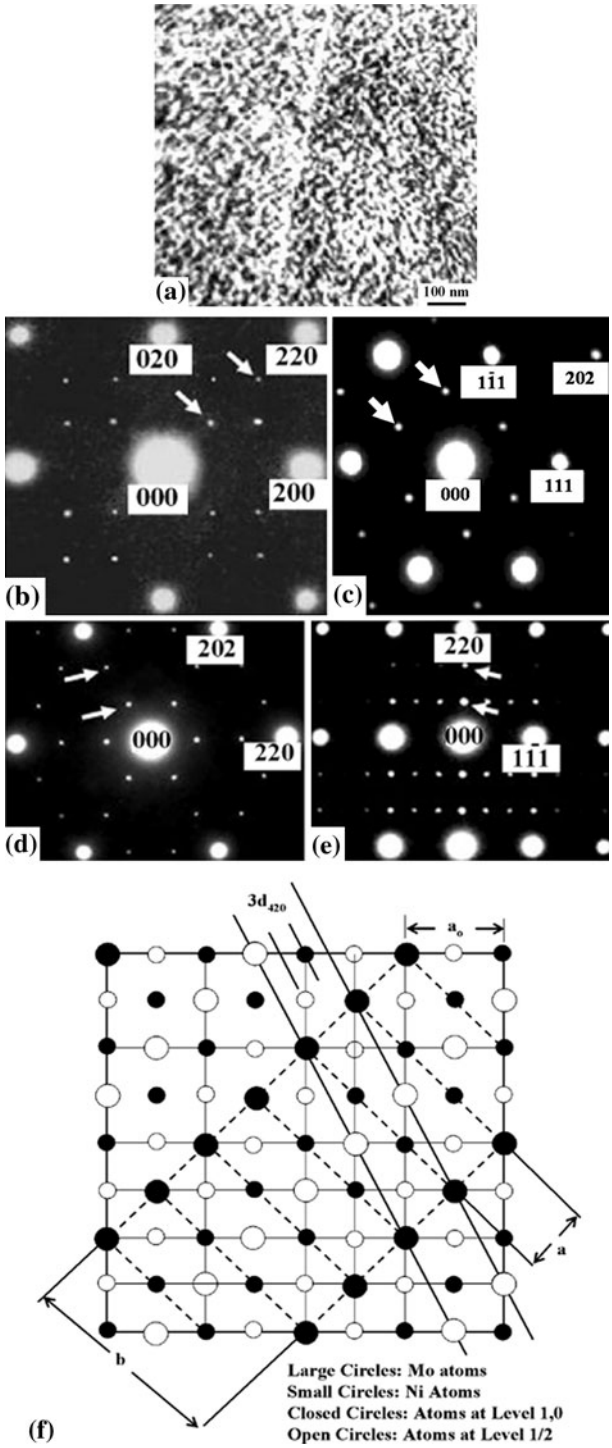

Fig. 3 Effect of 24 h of thermal aging at 700 °C on the structural features of the $Ni_2(Cr,Mo)$ alloy. (a) Bright-field TEM image showing "mottled" contrast characteristic of a large volume fraction of ultrafine particles. (b) ⟨00⟩ diffraction pattern. (c) ⟨110⟩ diffraction pattern. (d) ⟨111⟩ diffraction pattern. (e) ⟨112⟩ diffraction pattern. (f) A schematic illustrating the crystallographic features of the *fcc-to-Pt_2Mo-type* superlattice transformation noting that Mo atoms can be replaced by Cr atoms

structure is subdivided into six crystallographically equivalent variants of the Pt_2Mo-type superlattice assuming the morphology of nanoscale crystals. This is demonstrated in the dark-field TEM images of Fig. 4. Each of the images of Fig. 4 is formed

with a 1/3 ⟨220⟩ reflection bringing into contrast one variant of the Pt_2Mo-type superlattice. After up to at least 100 h of aging at 700 °C, the ordered crystals were found to maintain a nanoscale size (at least one of the dimensions is >100 nm). This ultrafine structure of ordered crystals and the corresponding high ductility are expected to be beneficial in terms of resisting crack propagation and improving fracture toughness.

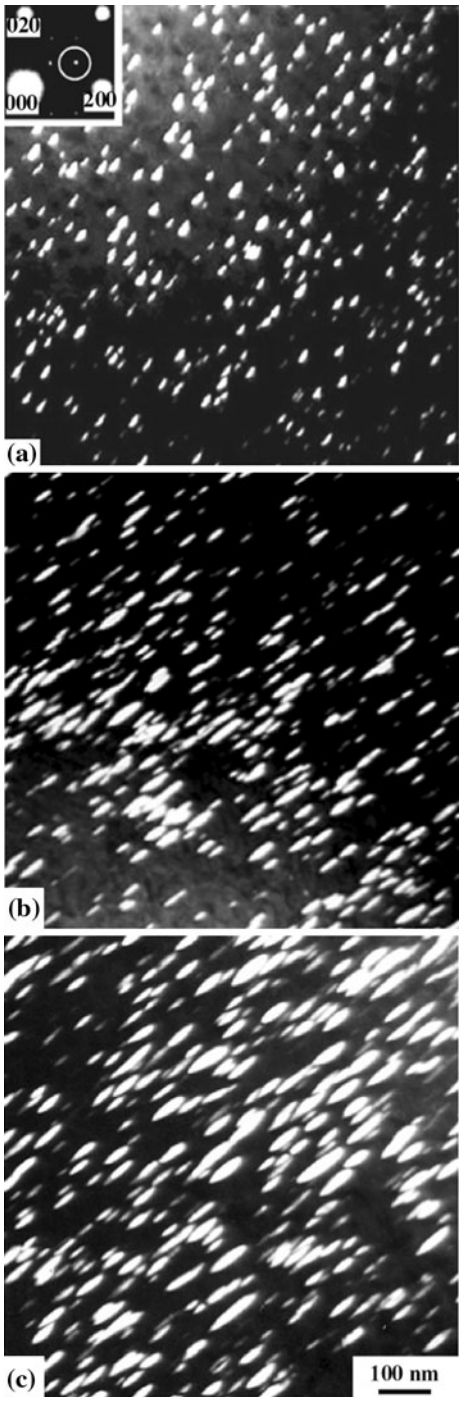

Fig. 4 Dark-field TEM images formed with 1/3 ⟨220⟩ superlattice reflections to illustrate the morphology of ordered crystals of the Pt_2Mo-type superlattice as a function of thermal aging time at 700 °C (a) 8 h (the inset is a section of the ⟨001⟩ diffraction pattern; the encircled 1/3 ⟨220⟩ superlattice reflection is used to form the image). (b) 24 h. (c) 100 h

3.4 Properties of $Ni_2(Cr,Mo)$ in the Long-Range Ordered State

Figure 5 shows the mean coefficient of thermal expansion of long-range ordered $Ni_2(Cr,Mo)$ in the range of room temperature to 700 °C in comparison with of INCOLOY® alloy 909 (38.3 Ni-41.4 Fe-12.9 Co-5.1 Nb-1.56 Ti-0.42 Si-0.1 Cr-0.05 Al-0.005 C in wt.%), which is well known for its low-thermal expansion characteristics (Ref 10) (INCOLOY® is registered trademark of Special Metals Corporation Group of Companies). As can be seen, the thermal expansion characteristics of $Ni_2(Cr,Mo)$ are comparable to those of alloy 909, however, the intermetallic is characterized by ultrahigh strength combined with high ductility and other useful properties as demonstrated below.

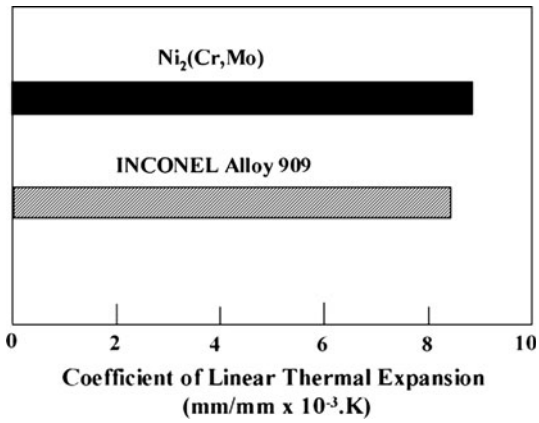

Fig. 5 Comparative coefficient of linear thermal expansion of INOCLOY® alloy 909 and $Ni_2(Cr,Mo)$ intermetallic in the range of room temperature to 700 °C

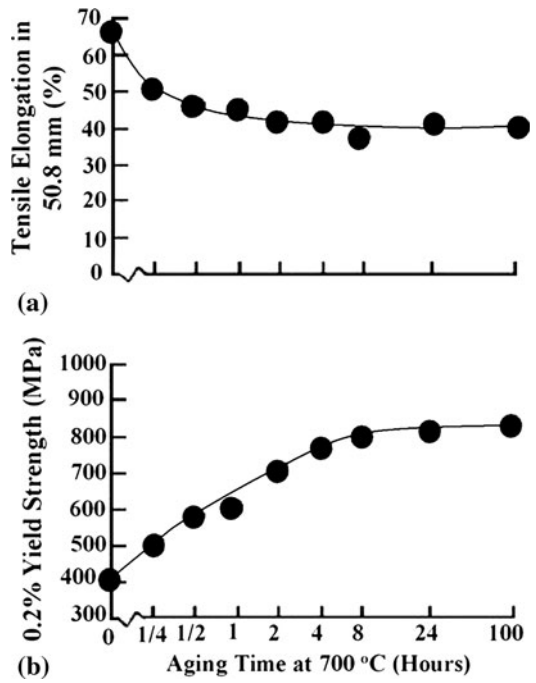

Fig. 6 Effect of thermal aging time at 700 °C on the room temperature tensile properties. (a) Tensile elongation in 50.8-mm gage length. (b) Corresponding 0.2% yield strength

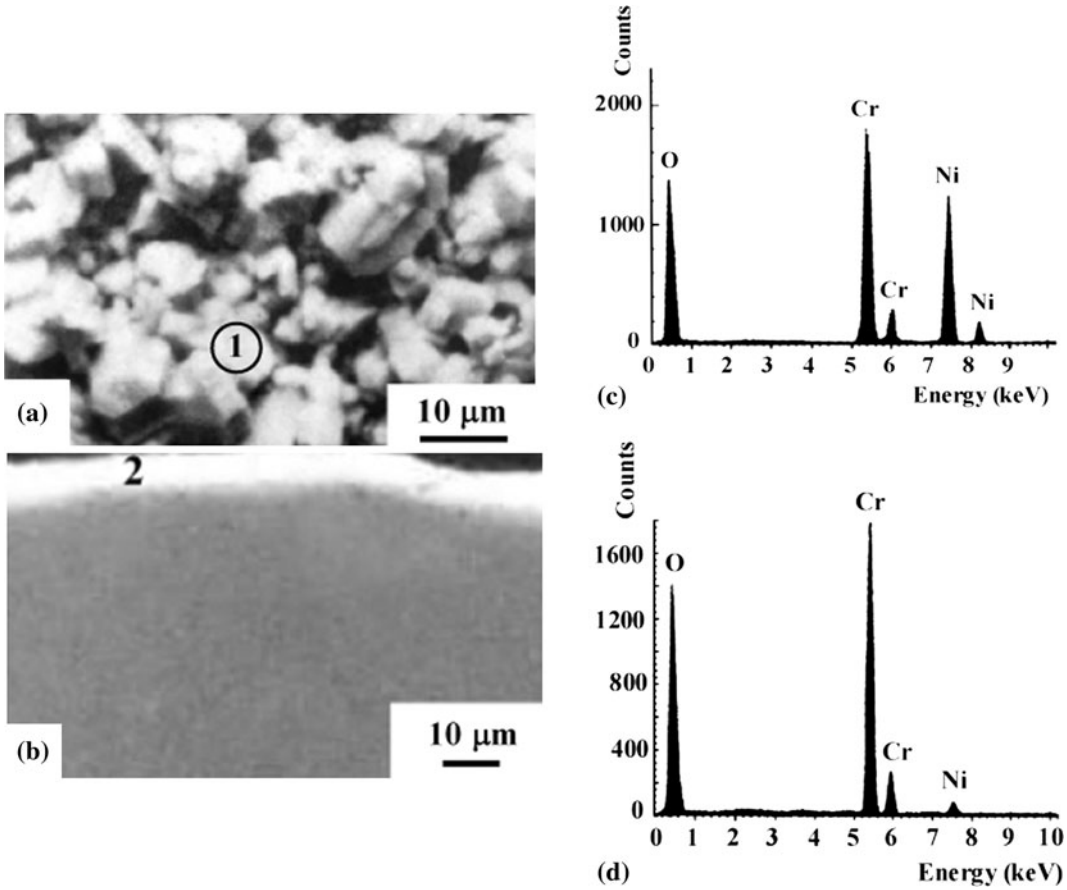

Fig. 7 An example illustrating the oxidation behavior of $Ni_2(Cr,Mo)$ intermetallic after 100 h of thermal exposure at 700 °C in air with an 8 h cycling period to room temperature. (a) Secondary electron SEM image showing the surface morphology of the scale. (b) Secondary electron SEM image of a cross section along the scale and into the substrate. (c) Energy dispersive x-ray spectrum derived from the region marked 1 in (a) to show the elemental composition of the outer scale layer. (d) Energy dispersive x-ray spectrum derived from the region marked 2 in (b) to illustrate the elemental composition of the inner scale layer

The effect of thermal aging at 700 °C on room temperature tensile properties is shown in Fig. 6. It is observed that after 100 h of aging, the material retained about 70% of its initial tensile ductility; however, the 0.2% yield strength was nearly doubled reaching about 820 MPa with a corresponding ductility of about 40%. These changes in tensile strength were correlated with long-range ordering to a Pt_2Mo-type superlattice as shown in Fig. 3 and 4.

Figure 7 illustrates morphology and elemental composition of the oxide scale developed by $Ni_2(Cr,Mo)$ intermetallic after 100 h of thermal exposure in air at 700 °C with an 8 h cycling period to room temperature. The morphology of the surface scale is shown in the secondary electron SEM image of Fig. 7(a) indicating the presence of an outer and inner layers of oxide. Along the cross section, the inner layer with a thickness of about 5 μm was well adhered to the substrate as shown in Fig. 7(b). Energy dispersive x-ray spectra derived from the outer scale layers such as the region marked 1 in Fig. 7(a) showed that the metallic constituents were Ni and Cr suggesting a spinel of the type $NiCr_2O_4$. In contrast, Cr was the predominant metallic constituent of the inner oxide layer consistent with Cr_2O_3 as expected. Evidently, the inner protective layer of Cr_2O_3 was overgrown by the less protective spinel. In addition to the above useful combination of properties, long-range ordered $Ni_2(Cr,Mo)$ was found to deform by twinning rather than by slip as shown below.

3.5 Deformation Mechanism of $Ni_2(Cr,Mo)$ in the Long-Range Ordered State

Figure 8(a) is a bright-field TEM image showing a typical deformation substructure of $Ni_2(Cr,Mo)$ intermetallic corresponding to 15% tensile elongation at room temperature. It is observed that the substructure contains a high density of nanoscale ⟨111⟩ twins resulting in heavy streaking of diffraction maxima in the corresponding ⟨110⟩ diffraction pattern shown in Fig. 6(b). This behavior could be correlated with the crystallographic features of the Pt_2Mo-type superlattice. It can readily be shown from the atoms arrangement on {111} planes illustrated in Fig. 6(c) that 10 of the 12 {111} ⟨110⟩ slip systems in the parent fcc structure become energetically unfavorable modes of deformation in the Pt_2Mo-type superlattice of $Ni_2(Cr,Mo)$. In contrast, 10 of the 12 {111} ⟨112⟩ twin system in the fcc structure remain energetically favorable in the superlattice. Therefore, twining rather than slip becomes the predominant deformation mechanism of the $Ni_2(Cr,Mo)$ intermetallic, which enhances its plasticity.

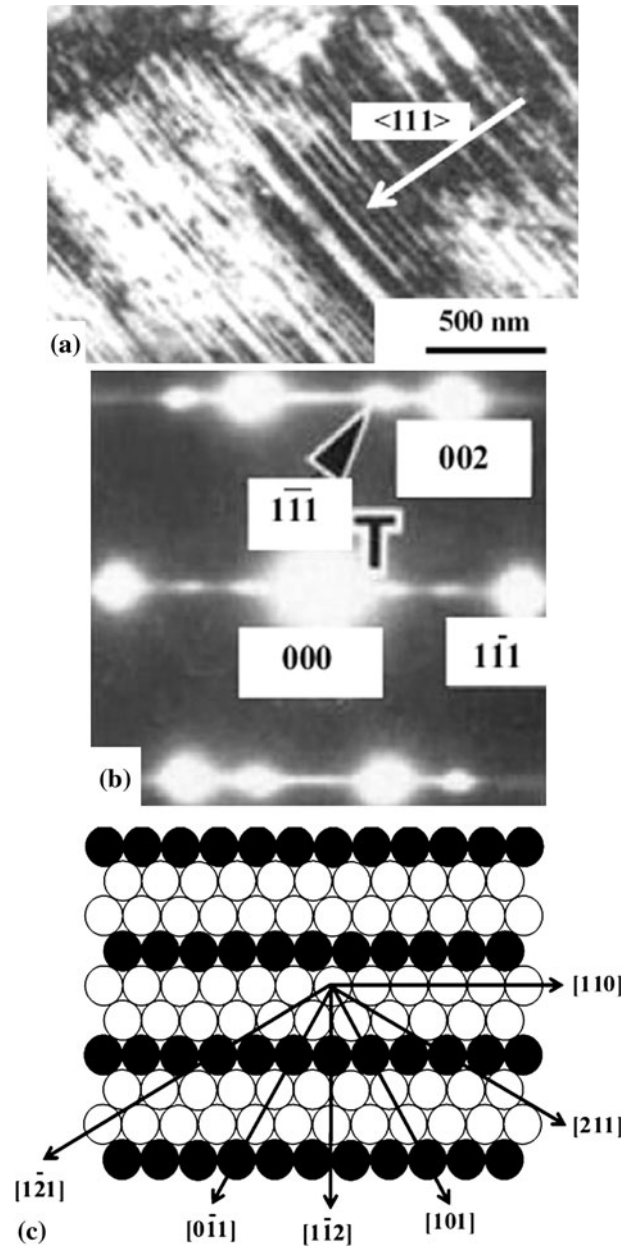

Fig. 8 Deformation behavior of the Ni_2Cr,Mo intermetallic (specimen given 15% tensile elongation at room temperature after 24 h of thermal aging at 700 °C). (a) Bright-field TEM image showing nanoscale ⟨111⟩ twins in the deformation substructure. (b) Corresponding ⟨110⟩ twin diffraction pattern, the heavy streaking of the diffraction maxima is due to the thinness of the twins. (c) Atoms arrangement on the {111} planes of the Pt_2Mo-type superlattice (Ni: open circles, Mo/Cr: closed circles)

4. Conclusions

Thermal aging at 700 °C of a Ni-Cr-Mo alloy with an approximate composition of $Ni_2(Cr,Mo)$ is found to result in the subdivision of each grain of the high-temperature fcc phase into nano-sized crystals of six crystallographically equivalent variants of a Pt_2Mo-type superlattice. Experiment shows that the nanostructured superlattice possesses a potentially useful combination of properties for high-temperature applications particularly gas turbine seal rings including a combination of high strength and high ductility in addition to adequate oxidation resistance and low-thermal expansion characteristics. The combination of enhanced plasticity due to deformation by twinning, low-thermal expansion characteristics, and high resistance to crack propagation are expected to enhance fatigue life minimizing the incident of thermal fatigue, which is shown to be an important mode of failure of gas turbine seal rings.

Acknowledgments

It is a pleasure to acknowledge the continued support of King Fahd University of Petroleum & Minerals as well as the Saudi Ministry of Higher Education.

References

1. H. Saracvanamuttoo, G. Rogers, and H. Cohen, *Gas Turbine Theory*, 6th ed., Pearson Education Ltd, Essex, 2009, p 445–450
2. M.P. Boyce, *Gas Turbine Engineering Handbook*, Elsevier, Oxford/Burlington, MA, 2006, p 549–553
3. D. Kay. *Honeycomb Brazing Essentials for Successful Use as Turbine Seals Industrial Heating*, November 1 Issue (2003)
4. R.W. Cahn, Intermetallics: New Physics, *Contemp. Phys.*, 2001, **42**(6), p 365–375
5. H.M. Tawancy, Long-Range Ordering: An Approach to Synthesize Nanoscale Superlattices with High Strength and High Ductility, *Mater. Sci. Forum* (2010), **633/634**, p 421–435
6. K.A. Gschneidner et al., The Influence of Electronic Structure on the Ductile Behavior of B_2 CsCl-Type Intermetallics, *Acta Mater.*, 2009, **57**, p 5876–5881
7. P.R. Swann, Dislocation Arrangements in Face-Centered Cubic Materials, *Electron Microscopy and Strength of Crystals*, G. Thomas and J. Washburn, Ed., Wiley, New York, 1963, p 131–181
8. H.M. Tawancy and M.O. Aboelfotoh, Experimental Observation of Transient Phases During Long-Range Ordering in a Ni-Mo Alloy, *Phys. Stat. Solid. A Appl. Res.*, 1987, **99**(2), p 461–466
9. H.M. Tawancy, Formation of DO22 Superlattice During Long-Range Ordering to Ni_4Mo in a Ni-Mo Alloy, *Scr. Met.*, 1984, **18**(4), p 343–346
10. INCOLOY® Alloy 909, September 4, 2004, Publication Number SMC-077, Special Metals Corporation, Princeton, KY